Smart Structures and Systems, *Vol. 28, No. 1 (2021) 105-119*
https://doi.org/10.12989/sss.2021.28.1.105

Advancing real-time hybrid simulation for coupled nonlinear soil-isolator-structure system

Hongwei Li [1], Amin Maghareh [2], Johnny W.C. Uribe [3], Herta Montoya [3], Shirley J. Dyke [2] and Zhaodong Xu*[1]

[1] *Key Laboratory of C&PC Structures of the Ministry of Education, Southeast University, Nanjing, 210096, China*
[2] *School of Mechanical Engineering, Purdue University, West Lafayette, IN 47907, USA*
[3] *Lyles School of Civil Engineering, Purdue University, West Lafayette, IN 47907, USA*

(*Received August 2, 2020, Revised March 10, 2021, Accepted March 20, 2021*)

Abstract. Experiments involving soil-structure interaction are often constrained by the capacity and other limitations of the shake table. Additionally, it is usually necessary to consider different types of soil in experiments. Real-time hybrid simulation (RTHS) offers an alternative method to conduct such tests. RTHS is a cyber-physical testing technique that splits the dynamic system under investigation into numerical and physical components, and then realistically couples those components in a single test. A limited number of previous studies involving soil-structure interaction have been conducted using RTHS, with a focus on linear models and systems. The presence of isolators was not considered in these studies to the authors' best knowledge. Herein, we aim to advance the understanding of the RTHS method by developing and demonstrating its use for nonlinear soil-isolator-structure systems. A sliding mode controller able to deal with both system nonlinearities and wide range of potential uncertainties in such tests is designed and validated using a nonlinear shake table with a nonlinear specimen. By simply changing the numerical model and using the same controller and experimental setup, different soil types and ground motions can readily be considered with this approach. Numerical and RTHS results are compared for verification purposes.

Keywords: nonlinear dynamics; nonlinear shake table; real-time hybrid simulation; sliding isolation; sliding mode control; soil-isolator-structure interaction

1. Introduction

A number of past studies have used large shake tables to examine the behavior of coupled soil-structure systems (Luco *et al*. 1988, Gueguen and Bard 2005, Aldaikh *et al*. 2015, Zhuang *et al*. 2019). However, conducting large- and full-scale experiments is costly and time-consuming. Enclosing a sufficient amount of soil in a soil-box is typically required to adequately emulate the soil-structure interaction (SSI) effects (Todorovska 2002, Kabeyasawa 2008, Ebeido *et al*. 2018). Because this greatly increases the payload on the shake table, this requirement does impose limitations on the size of the superstructure. In addition, there is a boundary beyond which the scale cannot be reduced further, ensuring that the soil properties are compatible with the scaling laws. Clearly, a significant amount of preparatory work is needed to set up a single experiment, and then once it is in place, that configuration may not be suitable to consider a variety of soil types. Only a few shake tables around the world meet all of these requirements and support such testing. Complementary testing methods that can inform such experiments and thus allow researchers to focus their experimental efforts on the most relevant and informative experiments are needed.

*Corresponding author, Professor,
E-mail: zhdxu@163.com

RTHS provides an alternative means to conduct such experiments. RTHS is a cyber-physical testing method typically used for structural testing that includes rate dependencies (Blakeborough *et al*. 2001). A structural system is divided into numerical (computational) and physical (experimental) components, which can greatly reduce the costs and time involved in design, fabrication, and execution of an experiment (Gao *et al*. 2013, Gomez *et al*. 2015, Chen *et al*. 2019). In RTHS, certain challenges are also present. First, the interface conditions between the numerical and physical specimens should be enforced. Also, transfer system dynamics, time delay/lag and control-structure interaction effects (Dyke *et al*. 1995) should be carefully handled. These challenges of RTHS have been thoroughly discussed in the literature (Chae *et al*. 2013, Maghareh *et al*. 2014, 2017, Wang *et al*. 2014, Ou *et al*. 2017, Chen and Chen 2020). Hydraulic or electric-powered actuators are generally used as transfer systems in RTHS due to their ability to respond relatively quickly and with a large force capacity.

A select group of researchers have adopted shake tables as the transfer system in RTHS experiments. For example, uniaxial shake tables have been used to reproduce inter-story motions in RTHS to evaluate buildings subjected to earthquakes. Here, using acceleration feedback, a proportional controller (Nakata and Stehman 2014) and a linear quadratic Gaussian controller (Zhang *et al*. 2016, 2017) were designed to drive the shake table. As discussed

ISSN: 1738-1584 (Print), 1738-1991 (Online)

by the authors, the reliable bandwidth of the controllers was limited to 6 Hz (Nakata and Stehman 2014) and 5 Hz (Zhang *et al*. 2016, 2017). In previous work on SSI using RTHS (Wang *et al*. 2011, Zhou *et al*. 2014), the soil was represented with a two degree-of-freedom (DOF) linear lumped-mass model (Wang *et al*. 2011) and a 132-DOF finite element model (Zhou *et al*. 2014). A displacement-based shake table controller was used in these studies. Later, an acceleration-based controller was adopted to study SSI effects using RTHS (Guo *et al*. 2016). However, these studies consider only a linear, single-variable tracking controller. This approach may have limitations in achieving good tracking performance as the test specimen becomes more complex or nonlinear. This approach may also have modest performance when seeking to track both displacement and acceleration at the same time or to control nonlinear transfer systems. Thus, methods are needed that can accommodate nonlinear shake table dynamics while also exhibiting robust tracking performance for both displacement and acceleration. Additionally, although there are abundant studies examining SSI with base isolators in the superstructures (Constantinou and Kneifati 1988, Spyrakos *et al*. 2009, Tsai *et al*. 2016, Neethu and Das 2019), no RTHS of soil-isolator-structure coupled systems can be found in literature to the authors' best knowledge. It is worthwhile to conduct RTHS for the systems including base isolators because they are widely adopted in engineering practice.

In this paper, we focus on advancing the theory and capacity of RTHS methods toward their use for experimentation involving nonlinear soil-isolator-structure system. A shake table with nonlinear behavior serves as the transfer system to enforce interface conditions between the numerical (foundation/soil) and the physical (super-structure) components. A nonlinear numerical model is established as the reference model to verify the RTHS results. The foundation and the soil comprise the numerical component in the RTHS. The simplified, linear sway-rocking model is applied to describe a range of soils, and we show that three types of soil (soft, medium, and dense) can be considered with a single experimental setup. The physical component consists of a superstructure which is a 2-DOF linear shear frame equipped with four geometric nonlinear rolling isolators. The shake table exhibits highly nonlinear behavior due to friction. An approach for designing a robust model-based sliding mode controller is developed by incorporating necessary considerations and adaptations of the friction and uncertainties for the nonlinear shake table. A set of problem-specific evaluation criteria are defined and computed to quantitatively evaluate the controller tracking performance as well as the RTHS performance as compared with the reference model.

2. Nonlinear reference model

Consider the system shown in Fig. 1(a), consisting of a shear type frame, nonlinear rolling isolators, a foundation and soil layers between the foundation and solid rock. The input to the system is the ground motion from the solid rock. The system has three subsystems: (a) foundation/soil subsystem; (b) base subsystem; (c) frame subsystem. The nonlinear reference model is presented in this section.

2.1 Formation of the reference model

The system shown in Fig. 1(a) is represented as a nonlinear coupled system as shown in Fig. 1(b), where $\ddot{x}_g$ is the ground motion, x_0 is the foundation displacement relative to the ground (solid rock), x_b, x_1 and x_2 are displacements of the base, first floor and second floor, relative to the foundation. The base mass m_b includes the top part of the isolators, the foundation mass m_0 includes the bottom part of the isolators. k_0 and c_0 are the stiffness and damping coefficients of soil. k_i and c_i $(i = 1, 2)$ are the stiffness and damping coefficients of the frame. Detailed descriptions of the reference model for each subsystem are presented in follows.

(a) Foundation/soil subsystem

The linear sway-rocking (SR) model is one of the common models used for the SSI (Ghahari *et al*. 2013, Pioldi *et al*. 2017). In the SR model, translational and rotational stiffness and damping values are adopted, which are determined based on the shear modulus, Poisson's ratio, mass density and shear-wave velocity of the adopted soil

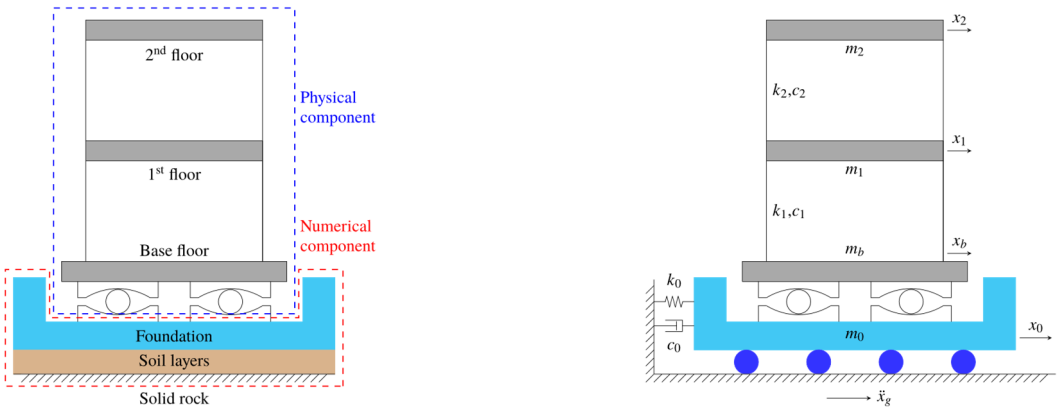

(a) Structure-isolator-soil system (b) Reference model of the system

Fig. 1 The studied structure-isolator-soil system and its reference model

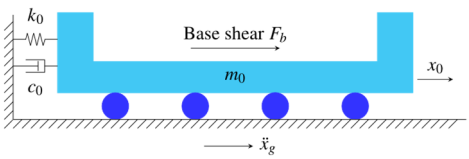

Fig. 2 Foundation/soil subsystem

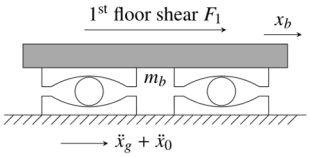

Fig. 3 Base subsystem

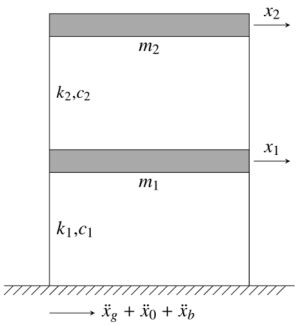

Fig. 4 Shear frame subsystem

(Pioldi *et al*. 2017). Depending on the scope and complexity of the study, the soil stiffness and damping values may be defined as frequency-dependent (Pais and Kausel 1988) or constant (Pioldi *et al*. 2017) values. Here we assume they are constant. The rotational stiffness is usually much larger than the translational stiffness, therefore the foundation rotation only becomes evident when the superstructure has a high center of mass. The tested frame in this paper has only two floors which might cause minor foundation rotation. And given the fact that the used shake table cannot generate rotational movements, the rotational effects of SSI is ignored here. Note that this study is focused on advancing the use of RTHS techniques to enable SSI studies, rather than exploring the influence of the soil in detail. The simplified SR model is adopted here more for the purpose of demonstrating and evaluating the proposed RTHS technique. However, the RTHS technique is not limited to the selected SSI model. More sophisticated SSI models which include rotational and nonlinear effects could certainly be considered using the proposed RTHS technique if a shake table with rotational (pitch) capabilities were available and if the computational needs for complex soil models were available.

Based on the simplified SR model described above, Fig. 2 shows the free body diagram of the foundation/soil subsystem. The equation of motion (EOM) of the foundation is

$$m_0\ddot{x}_0 + c_0\dot{x}_0 + k_0x_0 = -m_0\ddot{x}_g + F_b, \tag{1}$$

where F_b is the base shear force.

(b) Base subsystem

The nonlinearity of the coupled soil-isolator-structure system is in the base subsystem. Besides rubber bearings that are the most commonly used base isolators, friction and rolling (ball) pendulum isolators are also widely adopted in base isolation systems due to the pendulum mechanisms involved (Jangid 2005, Harvey and Gavin 2013, Calhoun and Harvey 2018). The isolator of interest in this study is the highly geometric nonlinear rolling isolator shown in Fig. 3, where the rolling surface of the isolators is a circular arc with radius R_c, and the radius of the rolling ball is r.Defining the effective radius $R = 2(R_c - r)$ and according to the Lagrange's equation, the EOM of the isolated base is

$$\frac{m_bR^2\ddot{x}_b}{R^2 - x_b^2} + c_b\dot{x}_b + \frac{m_bR^2x_b\dot{x}_b^2}{(R^2 - x_b^2)^2} + \frac{(m_1 + m_2 + m_b)gx_b}{\sqrt{R^2 - x_b^2}} = m_b - (\ddot{x}_g + \ddot{x}_0) + F_1, \tag{2}$$

where, c_b is the damping coefficient combining all the isolators, $g = 9.8\ \mathrm{m/s^2}$ is the gravitational acceleration, and F_1 is the shear force at the first floor of the frame. Note that the non-conservative forces (nonlinear damping force, friction, etc.) are simplified as a single damping force $c_b\dot{x}_b$ see the second term in Eq. (2). As discussed later, this simplification of the base model is a main contributor to the RTHS error.

The base shear is given by

$$F_b = F_1m_b - (\ddot{x}_g + \ddot{x}_0 + \ddot{x}_b). \tag{3}$$

(c) Frame subsystem

According to Fig. 4, the EOM of the 2-DOF frame is

$$\mathbf{M}_s\ddot{\mathbf{x}}_s + \mathbf{C}_s\dot{\mathbf{x}}_s + \mathbf{K}_s\mathbf{x}_s = -\mathbf{M}_s\iota_s(\ddot{x}_g + \ddot{x}_0 + \ddot{x}_b) \tag{4}$$

where

$$\boldsymbol{x}_s = [x_1 - x_b, x_2 - x_b]^{\mathrm{T}} \tag{5}$$

and

$$\mathbf{M}_s = \begin{bmatrix} m_1 & 0 \\ 0 & m_2 \end{bmatrix}, \quad \mathbf{C}_s = \begin{bmatrix} c_1 + c_2 & -c_2 \\ -c_2 & c_2 \end{bmatrix}, \quad \iota_s = [1,1]^{\mathrm{T}}, \quad \mathbf{K}_s = \begin{bmatrix} k_1 + k_2 & -k_2 \\ -k_2 & k_2 \end{bmatrix}, \tag{6}$$

The first floor shear force is given by

$$F_1 = -m_1(\ddot{x}_g + \ddot{x}_0 + \ddot{x}_1) - m_2(\ddot{x}_g + \ddot{x}_0 + \ddot{x}_2). \tag{7}$$

2.2 Comparison with the linearized model

If the movement of the isolated base is relatively small ($x_b \ll R$), the rolling isolators can be approximated by a linear damper and a linear spring with the damping coefficient $\mathrm{c_b}$ and stiffness

$$k_b = (m_1 + m_2 + m_b)\, g/R. \tag{8}$$

Thus, the complete coupled soil-isolator-structure system can be represented with a linearized model. The EOM for the linearized model is

$$\mathbf{M}_l\ddot{\mathbf{x}}_l + \mathbf{C}_l\dot{\mathbf{x}}_l + \mathbf{K}_l\mathbf{x}_l = \mathbf{M}_l\iota_l\ddot{x}_g, \tag{9}$$

where

$$\boldsymbol{x}_l = [x_{0l}, x_{bl} + x_{0l}, x_{1l} + x_{0l}, x_{2l} + x_{0l}]^{\mathrm{T}}, \tag{10}$$

and

$$\mathbf{M}_l = \begin{bmatrix} m_0 & 0 & 0 & 0 \\ 0 & m_b & 0 & 0 \\ 0 & 0 & m_1 & 0 \\ 0 & 0 & 0 & m_2 \end{bmatrix}, \quad \mathbf{C}_l = \begin{bmatrix} c_0 + c_b & -c_b & 0 & 0 \\ -c_b & c_b + c_1 & -c_1 & 0 \\ 0 & -c_1 & c_1 + c_2 & -c_2 \\ 0 & 0 & -c_2 & c_2 \end{bmatrix},$$
$$\iota_l = [1,1,1,1]^{\mathrm{T}}, \quad \mathbf{K}_l = \begin{bmatrix} k_0 + k_b & -k_b & 0 & 0 \\ -k_b & k_b + k_1 & -k_1 & 0 \\ 0 & -k_1 & k_1 + k_2 & -k_2 \\ 0 & 0 & -k_2 & k_2 \end{bmatrix}, \tag{11}$$

x_{0l}, x_{bl}, x_{1l} and x_{2l} are the displacements of foundation, base, first floor and second floor in the linearized model, which are defined similar to x_0, x_b, x_1 and x_2 in Fig. 1(b) for the reference model.

The responses of this linearized model are compared with those of the nonlinear reference model. For both models, the effective radius is $R = 5.62$ cm. Other parameters are listed in Table 1. Note that these parameters are also used in the RTHS, and dense soil type is selected for the comparison. Detailed information and how to obtain these parameters will be discussed in Section 3.

Table 1 Parameters of the linearized model and the reference model

	Mass [kg]	Stiffness [N/m]	Damping [Ns/m]
Foundation/soil	10	5740	662
Base	6.4	1300	7.84
First floor	0.49	2909	2.0
Second floor	0.56	3387	0.5

*Note: the base stiffness is for the linearized model only

A band-limited white noise (BLWN) with a cutoff frequency of 10 Hz and a duration of 30 s is used as the ground displacement input. The ground velocity and acceleration inputs are numerical derivatives of the displacement input. Define a general expression for the normalized root mean square error (NRMS) as

$$\mathrm{NRMS}(y, z) = \frac{\mathrm{RMS}(y - z)}{max(z) - min(z)} \times 100\%, \tag{12}$$

where RMS(·) represents the root mean square error, y and z are the two vectors to be compared and they have the same dimension. Thus, the differences between the reference model and the linearized model can be quantified using the criterion

$$J_b = \mathrm{NRMS}(x_b, x_{bl}). \tag{13}$$

Fig. 5 shows the base displacement responses when the power spectral density (PSD) of the BLWN input is 0.1 cm^2.The responses of two models are almost the same with $J_b = 0.28\%$. As the amplitude of the input increases, geometric nonlinearity becomes an important factor. In Fig. 6, there are significant discrepancies between the responses associated with the linearized and reference models and J_b increases to 7.32%. Here, the PSD of the BLWN input is 10 cm^2. Note that the excitation used in Fig. 6 is also used in the RTHS tests. Fig. 7 plots how J_b changes as a function of PSD of the BLWN input. It can be seen that J_b increases with PSD and J_b will be greater than 5% when PSD > 6.5 cm^2. The comparison with the linearized model shows the significance of the geometric nonlinearity in the reference model.

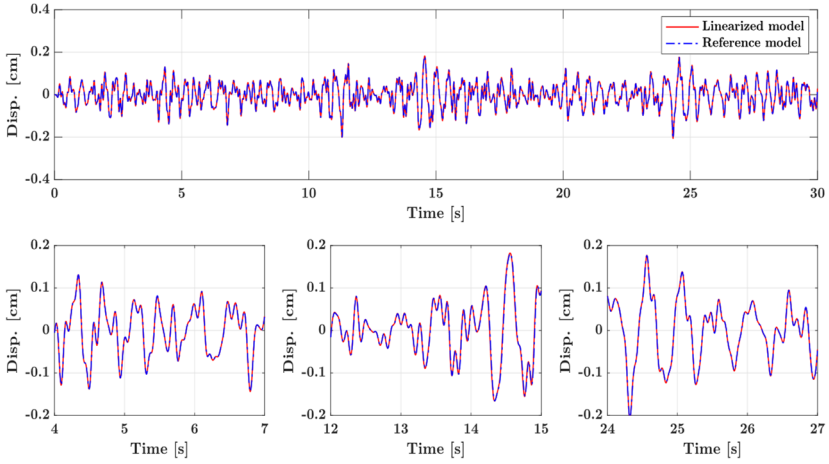

Fig. 5 Base displacement (relative to the foundation), PSD = 0.1 cm^2

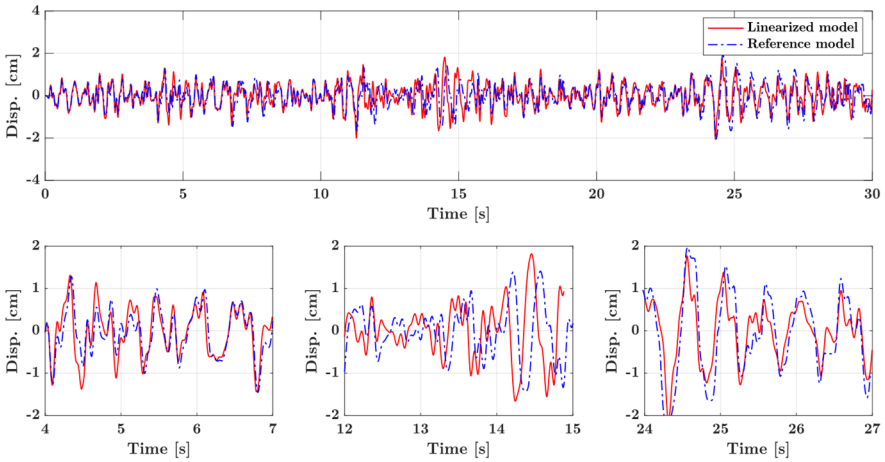

Fig. 6 Base displacement (relative to the foundation), PSD = 10 cm^2

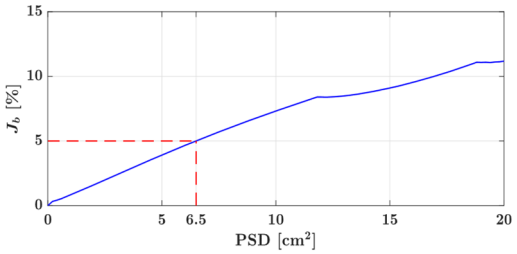

Fig. 7 Curve of J_b changing with PSD of the BLWN input

3. Real-time hybrid simulationy

In RTHS, foundation/soil subsystem is the numerical component, and the superstructure including the base and frame subsystems is the physical component. The RTHS setup, transfer system and the sliding mode control design are discussed in details in the following sections.

3.1 RTHS setup

To enforce the interface conditions between the numerical and physical components, a shake table located in the Intelligent Infrastructure Systems Laboratory (IISL) at Purdue University is used as the transfer system. This coupled dynamic system including shake table and physical component is called the *plant* hereafter, which is shown in Fig. 8.

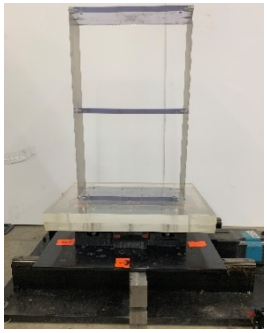

Fig. 8 Shake table and physical component

Fig. 9 shows the RTHS block diagram, where $\mathbf{x}_g$ is the input ground motion, x_d and $x_{\bar{m}}$ are designated and measured trajectories of the shake table, respectively, x_c is the command input to the shake table, and $F_{b\bar{m}}$ is the base shear calculated based on the measured accelerations. To be specific

$$\boldsymbol{x}_g = [x_g, \dot{x}_g, \ddot{x}_g], \tag{14}$$

$$\boldsymbol{x}_d = [x_d, \dot{x}_d, \ddot{x}_d] = [x_{0d}, \dot{x}_{0d}, \ddot{x}_{0d}] + \boldsymbol{x}_g, \tag{15}$$

$$\boldsymbol{x}_{\bar{m}} = [x_m, \dot{x}_{\bar{m}}, \ddot{x}_m], \tag{16}$$

$$F_{b\bar{m}} = -m_b\ddot{u}_{bm} - m_1\ddot{u}_{1m} - m_2\ddot{u}_{2m}, \tag{17}$$

where x_{0d} is the designated foundation displacement (relative to the ground), x_m is the measured absolute displacement of the shake table, $\ddot{u}_{bm}$, $\ddot{u}_{1m}$ and $\ddot{u}_{2m}$ are measured absolute accelerations of the base, first floor and second floor, respectively. Note that all variables with the subscript "m" means we can actually measure them in the test. However, variables with subscript "$\bar{m}$" such as $F_{b\bar{m}}$ and $\dot{x}_{\bar{m}}$ means they are calculated based on measured variables. For reasons of clarity and consistency, the variables that will be mentioned in the rest of the paper are absolute variables unless stated otherwise, because all measurements in the test are absolute values.

3.2 Transfer system

The uniaxial shake table plays the role of transfer system in this study. Its behavior is highly nonlinear due to friction in the shake table bearings. For the purpose of this

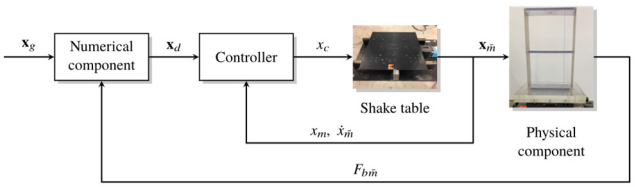

Fig. 9 RTHS block diagram

study, the way to model the shake table here is not to use a precise and complicated model to include all the nonlinear dynamics of the shake table, but to create a relatively simple nonlinear model which captures the essential dynamics. And by including a reasonable range of uncertainties on the model parameters, the shake table can be well represented using that model. The advantage of such nonlinear model with uncertainties is that it takes less control efforts without losing the control performance for the sliding mode controller. The shake table can be represented using the following model (Condori *et al*. 2020)

$$\ddot{x}_m = f(x_m) + dx_c, \tag{18}$$

where

$$f(x_m) = a\dot{x}_{\bar{m}} + bx_m + \gamma \tanh(\rho\dot{x}_{\bar{m}}). \tag{19}$$

In the above model, parameters a and b are associated with the linear damping and stiffness of the shake table, and the term $\gamma \tanh(\rho\dot{x}_{\bar{m}})$ with parameters γ and ρ denotes the nonlinear friction.

The nominal function for $f(\cdot)$ is

$$\hat{f}(\Delta) = \hat{a}\dot{\Delta} + \hat{b}\Delta + \hat{\gamma}\tanh(\rho\dot{\Delta}), \tag{20}$$

where $\hat{a}$, $\hat{b}$and $\hat{\gamma}$ are nominal values of a, b and γ. Parameters a, b and γ are assumed to be bounded in $[a_{min}, a_{max}]$, $[b_{min}, b_{max}]$ and $[\gamma_{min}, \gamma_{max}]$. Setting $\hat{a}$, $\hat{b}$and $\hat{\gamma}$ as the numerical means of the above bounds yields

$$\hat{a} = \frac{a_{max} + a_{min}}{2}, \quad \hat{b} = \frac{b_{max} + b_{min}}{2}, \quad \hat{\gamma} = \frac{\gamma_{max} + \gamma_{min}}{2}. \tag{21}$$

Therefore, the estimation error on $f(\cdot)$ is bounded by a function $\tilde{f}(\cdot)$

$$\begin{aligned} &| \hat{f}(\Delta) - f(\Delta) | \leq \tilde{f}(\Delta) \\ &= \tilde{a} | \dot{\Delta} | + \tilde{b} | \Delta | + \tilde{\gamma} | \tanh(\rho\dot{\Delta}) |, \end{aligned} \tag{22}$$

where

$$\tilde{a} = \frac{a_{max} - a_{min}}{2}, \quad \tilde{b} = \frac{b_{max} - b_{min}}{2}, \quad \tilde{\gamma} = \frac{\gamma_{max} - \gamma_{min}}{2}. \tag{23}$$

3.3 Sliding mode control system

The sliding mode control method is adopted due to the nonlinear nature of this plant. Let

$$e = x_m - x_d \tag{24}$$

be the tracking error in the shake table (foundation) displacement. The compact tracking error is defined as

$$E = \dot{e} + \lambda e, \tag{25}$$

where λ is a strictly positive constant (unit: 1/s). The goal of the controller is to keep the scalar E always tending to zero, which can be achieved by choosing the control law that satisfies (Slotine and Li 1991)

$$E\dot{E} \leq -\eta | E |, \tag{26}$$

Where η is a strictly positive constant (nondimensional). And with considering of uncertainties on the model parameters, the control law can be deduced as

$$x_c = \hat{d}^{-1}\hat{u}(x_m) - \hat{d}^{-1}\bar{k}(x_m)\text{sat}(E/\Phi), \tag{27}$$

where $\hat{d}$ is the nominal value of d. We assume that d is bounded in $[d_{min}, d_{max}]$. Since d represents the input gain, it is recommended to select $\hat{d}$ as the geometric gain of the bound of d

$$\hat{d} = \sqrt{d_{min} \cdot d_{max}}. \tag{28}$$

The first part $\hat{d}^{-1}\hat{u}(x_m)$ in Eq. (27) denotes the "perfect" command signal that would strictly achieve $E = 0$ if the shake table is governed by the nominal model, and the second part is the correction term considering the uncertainties on the shake table model. The detailed expressions of each term in Eq. (27) are

$$\hat{u}(\cdot) = -\hat{f}(\cdot) + \ddot{x}_d - \lambda\dot{e}, \tag{29}$$

$$\bar{k}(x_m) = k(x_m) - k(x_d) + \lambda\Phi/\beta, \tag{30}$$

$$k(\cdot) = \beta\left[\tilde{f}(\cdot) + \eta\right] + (\beta - 1) | \hat{u}(\cdot) |, \tag{31}$$

$$\beta = (d_{max}/d_{min})^{1/2}, \tag{32}$$

and Φ is the boundary layer surrounding the "surface" $E = 0$. The chattering in the control signal could be eliminated properly with the adoption of the saturation function of E and Φ (Li *et al*. 2021)

$$\text{sat}(E/\Phi) = \begin{cases} E/\Phi, & | E/\Phi | \leq 1 \\ \text{sgn}(E), & | E/\Phi | > 1' \end{cases} \tag{33}$$

where sgn is defined as follows

$$\text{sgn}(x) = \begin{cases} -1, & x < 0 \\ 0, & x = 0. \\ 1, & x > 0 \end{cases} \tag{34}$$

Fig. 10 shows how the boundary layer smooths the control command and a schematic drawing of the boundary layer along the sliding surface. The thickness of the boundary layer Φ can be tuned in real time in the test so that $\dot{E}$ always represents a first-order filter of E with bandwidth λ, thus Φ satisfies

$$\dot{\Phi} = \begin{cases} -\lambda\Phi + \beta k(x_d), & k(x_d) > \lambda\Phi/\beta \\ -\lambda\Phi/\beta^2 + k(x_d)/\beta, & k(x_d) \leq \lambda\Phi/\beta \end{cases}. \tag{35}$$

As stated previously, the shake table velocity $\dot{x}_{\bar{m}}$ cannot be measured directly. In this work, $\dot{x}_{\bar{m}}$ is calculated based on the shake table displacement x_m, which is

(a) $\mathrm{sgn}(E)$ and $\mathrm{sat}(E/\Phi)$ (b) Sliding surface and the boundary layer

Fig. 10 Control command interpolation within the time-varying boundary layer

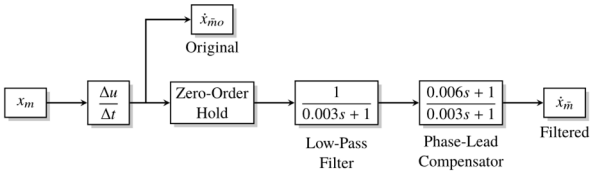

Fig. 11 Elimination of shake table velocity spikes

obtained directly from the digital encoder inside of the shake table. The encoder has a resolution of $\Delta x_m = 1/4000$ cm for the displacement measurement, leading to very high smoothness of x_m in time domain. However, the data processing in the test is executed using a fixed time step $\Delta t = 1/2048$ s. Therefore, if a first-order derivative of x_m is taken to obtain the shake table velocity, the resolution of the velocity is $\Delta x_m/\Delta t = 0.00512$ m/s, which cannot be ignored because it is comparable to the velocity values. Thus, the velocity would have noticeable spikes in time domain. To eliminate these spikes caused by the derivative operation, a low-pass filter together with a phase-lead compensator are adopted as shown in Fig. 11, where s is the Laplace variable.

Fig. 12 demonstrates one representative case showing the elimination of the velocity spike in a real data set. The solid line represents the velocity computed by differentiating the measured displacement x_m. Hereinafter this velocity is referred to as *original velocity*. It can be seen that there are a lot of spikes on the solid line and the values are integral multiples of the resolution 0.00512 m/s. The dash line represents the filtered and phase compensated velocity, which is defined as the *filtered velocity* and it is much smoother. It has been verified by the author that the elimination of velocity spikes can make the controller to perform better. Thus, the term $\dot{x}_{\bar{m}}$ is specified to be the filtered velocity of the shake table, and it will be used as the feedback of the controller.

4. Experimental setup and identification

This section presents the preparatory work before conducting the RTHS test. First, the experimental setup is introduced. And then, information or identifications of three subsystems and the transfer system are presented.

4.1 Experimental setup

The shake table uses a custom built servo-motor manufactured by SMI Technology to move a 46 cm × 46 cm top plate with a stroke of 15 cm. A digital encoder which measures the top plate displacement with a resolution of 1/4000 cm is built inside of the shake table. All the tests

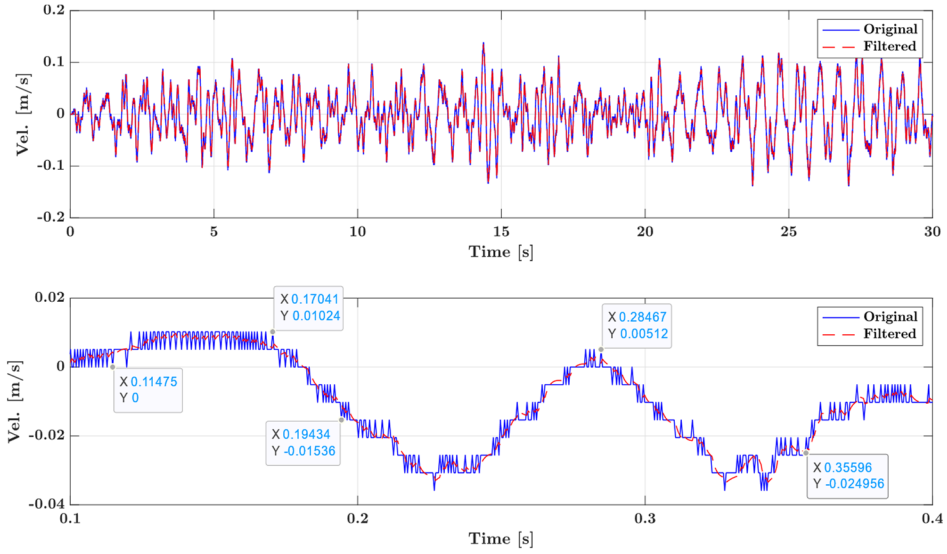

Fig. 12 A case of shake table velocity spikes elimination

are conducted at 2048 Hz using a commercial off-the-shelf sequential platform Speedgoat real-time kernel configured as a target PC equipped with a Core i5 3.5 GHz processor. Four accelerometers (model: PCB 33B40, frequency range: 0.5 to 3000 Hz) are attached at the shake table, base, first floor and second floor with wax to measure accelerations. The model of accelerometer power supply is PCB 483B08. A 16-bit NI-PCIe 6259 board with a NI SCB-68A 68 pin breakout connector is used as the data acquisition system. The integration and data processing are executed using the explicit fourth-order Runge-Kutta scheme (ode4) with a fixed time step $\Delta t = 1/2048$ s in Simulink, MATLAB 2013a.

4.2 Foundation/soil subsystem information

Three types of soil which are defined as soft, medium, and dense in the reference (Pioldi *et al*. 2017) are studied in this paper. The superstructure is small in size, therefore, to maintain the consistency in scaling between superstructure and foundation/soil, the foundation mass is selected as 10 kg to accommodate the superstructure. Then, according to the relationship between the soil and foundation parameters in the reference (Pioldi *et al*. 2017), and considering the shake table capacity (maximum displacement: ± 15 cm), a similarity ratio 2×10^{-5} is adopted here compared with the soil parameters listed in the reference (Pioldi *et al*. 2017). Table 2 summarizes the parameters for each soil type used in the present study.

4.3 Base subsystem identification

The base subsystem has four isolators. Figs. 13-14 show the design and layout. Polylactic acid filaments are used to 3D print the isolators and H buckles at the Innovation Design Center in Purdue University. Two isolators are restricted to move along the direction of analysis by the H type buckles. These, in turn, are connected to the shake table by bolts.

Table 2 Parameters of adopted soil types

Soil type	k_0 [N/m]	c_0 [Ns/m]
Soft	190.8	10.96
Medium	1800	34.6
Dense	5740	662

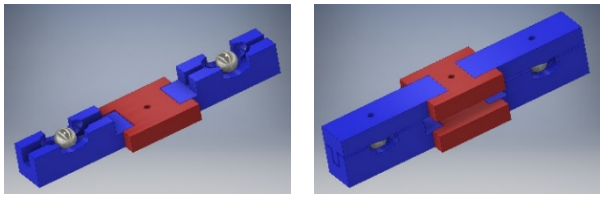

Fig. 13 3D sketches of the rolling isolators

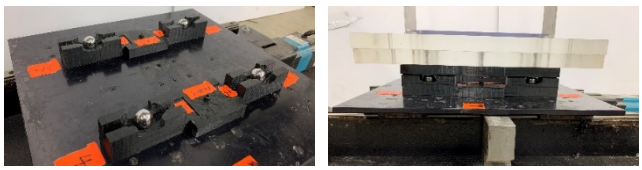

Fig. 14 The 3D printed rolling isolators

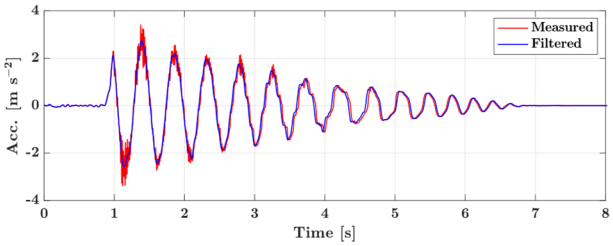

Fig. 15 Acceleration of the isolated base of free vibration

The radius of the rolling surface and the steel ball of the isolator are $R_c = 4$ cm and $r = 1.19$ cm (15/16 inches). Thus $R = 2(R_c - r) = 5.62$ cm. The base mass includes the top of part of the isolators is 6.4 kg. To identify the damping coefficient c_b in the base subsystem, several free vibration tests are conducted on the isolated base only (no frame on the top of the base) to extract the natural frequency ω_b and the damping ratio ξ_b. And then c_b is approximated using the equation $c_b = 2m_b\omega_b\xi_b$. Fig. 15 shows the base acceleration time-domain measurements for one of the free vibration tests. According to these tests, the average vibration period is identified as $T_b \approx 0.42$ s, which results in the average natural frequency: $\omega_b = 1/T_b \approx 2.40$ Hz. The damping ratio is determined using the logarithmic decrement method from Amp_p to $\text{Amp}_{\text{p+q}}$ over q cycles of motion (Chopra 2012)

$$\xi_b \approx \frac{1}{2\pi q} \ln\left(\frac{\text{Amp}_p}{\text{Amp}_{p+q}}\right). \tag{36}$$

Based on the tests, the average damping ratio is $\xi_b \approx 4.07$ %. Therefore $c_b = 2m_b\omega_b\xi_b = 7.84$ Ns/m. It is important to remark that the adoption of Eq. (36) indicates that the nonlinear effects such as nonlinear inertia, nonlinear restoring force, nonlinear damping, etc. are ignored when identifying the linear damping ratio ξ_b (and hence c_b). This simplification might be one reason contributing to the error between the numerical and RTHS results.

4.4 Frame subsystem identification

The measured masses for the first and second floors are 0.675 kg and 0.563 kg including the masses of the steel columns near each floor. To further identify the stiffness and damping values, the frame is mounted on the shake table and predefined BLWN signals with bandwidth of 30 Hz and different PSD: 5 cm^2, 10 cm^2 and 15 cm^2 (time duration is 180 s) are sent to the system to let the frame vibrate. A PI controller with the displacement feedback provided by a digital encoder is implemented in the test, with proportional and integral gains of 4 and 0.1, respectively. The accelerations of the shake table, first floor and second floor are measured, represented by $\ddot{u}_{0im}$, $\ddot{u}_{1im}$ and $\ddot{u}_{2im}$. The

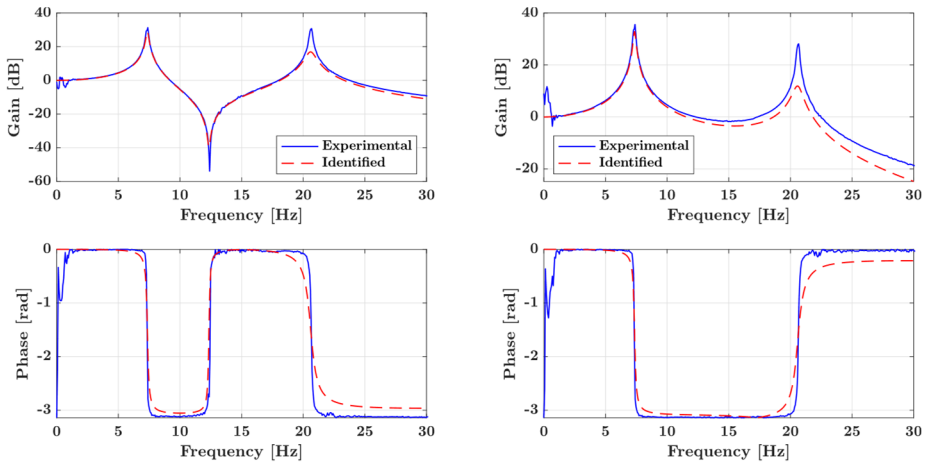

Fig. 16 Experimental and identified frequency responses, the left are for the first floor, the right are for the second floor

Table 3 Identified parameters of the frame

Floor	Mass [kg]	Stiffness [N/m]	Damping [Ns/m]
First	0.49	2909	2.0
Second	0.56	3387	0.5

transfer functions from $\ddot{u}_{0im}$ to $\ddot{u}_{1im}$ and $\ddot{u}_{2im}$ are given by the followings

$$TF_1(s) = \frac{\ddot{u}_{1im}(s)}{\ddot{u}_{0im}(s)} = \frac{1}{I}[m_2c_1s^3 + m_2k_1s^2 + H], \quad (37)$$

$$TF_2(s) = \frac{\ddot{u}_{2im}(s)}{\ddot{u}_{0im}(s)} = \frac{H}{I}, \quad (38)$$

where

$$H = c_1c_2s^2 + (c_1k_2 + c_2k_1)s + k_1k_2, \quad (39)$$

$$I = m_1m_2s^4 + [(m_1 + m_2)c_2 + m_2c_1]s^3 + [(m_1 + m_2)k_2 + m_2k_1]s^2 + H. \quad (40)$$

Based on the tests, the stiffness and damping of each floor can be determined by fitting the experimental transfer functions. Fig. 16 shows the experimental and identified frequency responses in terms of gain and phase. It can be seen that the responses at frequencies higher than 15 Hz cannot be captured well, especially around the second mode. In this study, the frame is considered as two lumped masses which are constant for the two modes, while modelling errors could arise because the masses of columns could alter the effective masses of each floor for different modes, especially for the higher mode (Harris and Piersol 2010). If the column mass were much smaller compared to the floor mass, such modelling error could be ignored. However, the mass ratio between the column and floor of the tested frame is relatively high (over 20%), therefore leads to the noticeable modelling error over 15 Hz as shown in Fig. 16. We will discuss that such modelling error is one noteworthy source of the errors between the RTHS and reference model results. Table 3 lists identified parameters of the frame. The effective masses for each floor have been slightly adjusted compared to the measured values.

4.5 Transfer system identification

To identify the shake table model parameters and the associated uncertainties, three conditions are considered here: 1. no additional mass on the shake table; 2. additional mass weighed 4.08 kg is attached on the shake table; 3. additional mass weighed 9.30 kg is attached on the shake table. Normally one would need to design a specific tracking controller for each RTHS case being considered. However, by experimentally determining the parametric uncertainty it is possible to design a single controller that will account for the variability in the test due to changes in the specimen. The identified system includes the PI controller (P gain is 4, I gain is 0.1) with displacement feedback that is used to stabilize the motor. The input command are selected as BLWN signals with bandwidth of 30 Hz and different PSD: 2.5 cm^2 and 3.5 cm^2 (time duration is 180 s). Table 4 lists the identified nominal values and uncertainties for parameters of the shake table model.

5. RTHS implementation and results

5.1 Excitations

Both a BLWN (cutoff frequency is 10 Hz, PSD is 10 cm^2) and a scaled El Centro earthquake are selected as excitations for the RTHS tests. The time/frequency of the El

Table 4 Identified parameters of the nonlinear shake table model

Parameter	a [s^{-1}]	b [s^{-2}]	γ [m/s^2]	d [s^{-2}]	ρ [s/m]
Nominal value	17.29	-47.40	-97.82	279.20	4.23
Uncertainty	(-21.0, -13.6)	(-73.7, -21.1)	(-112.0, -83.7)	(261.4, 298.2)	-

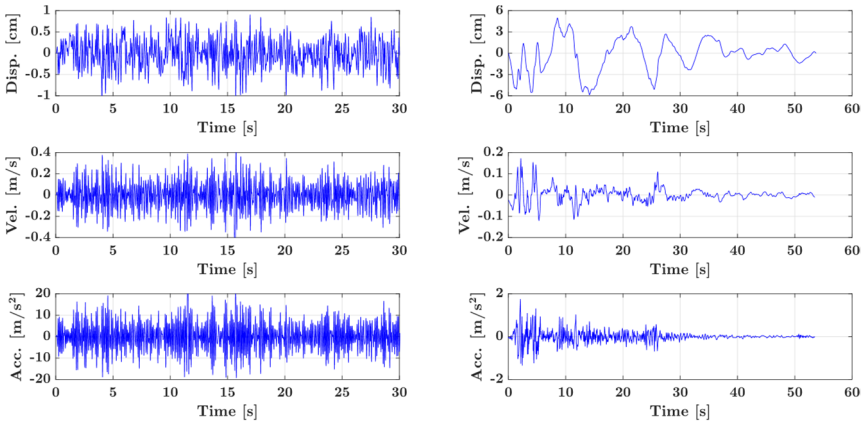

Fig. 17 Displacement, velocity, and acceleration of the ground excitations, left: BLWN, right: El Centro earthquake

Centro earthquake is not scaled, while the intensity of the earthquake is scaled down by one-half to meet the capacity of the shake table. Fig. 17 plots the time histories of the displacement, velocity, and acceleration for both excitations.

5.2 Observations

The measurements in the RTHS test are: 1) shake table displacement x_m; 2) shake table acceleration $\ddot{x}_m$; 3) base acceleration $\ddot{u}_{bm}$; 4) first floor acceleration $\ddot{u}_{1m}$; 5) second floor acceleration $\ddot{u}_{2m}$. The variables that are numerically obtained in real time in the RTHS test are: 1) shake table filtered velocity $\dot{x}_{\bar{m}}$; 2) shake table designated displacement x_d; 3) shake table designated velocity $\dot{x}_d$; 4) shake table designated acceleration $\ddot{x}_d$. Besides, to cut off the high frequency contents in the measured accelerations, the filtered variables $\ddot{x}_{mf}$, $\ddot{u}_{bmf}$, $\ddot{u}_{1mf}$ and $\ddot{u}_{2mf}$ based on $\ddot{x}_m$, $\ddot{u}_{bm}$, $\ddot{u}_{1m}$ and $\ddot{u}_{2m}$ are used for the evaluation.

5.3 Controller design

There are two parameters λ and η that need to be tuned for the sliding mode controller. η has little effect on the controller, it is selected as $\eta = 0.1$ in the tests. An efficient way to improve the performance of the controller is to increase λ to make it cover the bandwidth of the system response (Condori *et al.* 2020, Maghareh *et al.* 2020). However, increasing λ too much would make the controller aggressive and amplify the influence of the high frequency content of the measurements, thereby causing unnecessary control effort. It has been tested and verified by the authors that increasing λ to 400 s^{-1} (63.66 Hz) does not create noticeable high frequency content in the command signal x_c. In this way, the theoretical bandwidth of the controller is 63.66 Hz, which we believe would cover the possible high frequency responses excited in the RTHS tests. We have also tried to set $\lambda > 400$ s^{-1} and found the increase of the controller tracking performance is very limited. Therefore $\lambda = 400$ s^{-1} and $\eta = 0.1$ are adopted for the controller used in the RTHS test.

5.4 Evaluation criteria

To quantitatively evaluate the RTHS results and the performance of the sliding mode controller, nine RTHS evaluation criteria are defined here. Lower evaluation criteria indicate better performance. The first three criteria are called the **controller tracking criteria**. They are defined as the tracking errors of shake table displacement, velocity, and acceleration (referring to Eq. (12) for the function NRMS)

$$J_1 = \mathrm{NRMS}(x_d, x_m), \tag{41}$$

$$J_2 = \mathrm{NRMS}(\dot{x}_d, \dot{x}_{\bar{m}}), \tag{42}$$

$$J_3 = \mathrm{NRMS}(\ddot{x}_d, \ddot{x}_{mf}), \tag{43}$$

The next three criteria are defined as NRMS between the RTHS and reference model results for the shake table (foundation) displacement, velocity, and acceleration

$$J_4 = \mathrm{NRMS}(x_m, x_r), \tag{44}$$

$$J_5 = \mathrm{NRMS}(\dot{x}_{\bar{m}}, \dot{x}_r), \tag{45}$$

$$J_6 = \mathrm{NRMS}(\ddot{x}_{mf}, \ddot{x}_r), \tag{46}$$

where x_r , $\dot{x}_r$ and $\ddot{x}_r$ are the foundation absolute displacement, velocity, and acceleration obtained from the reference model. The last three criteria are defined as NRMS between results of RTHS and the reference model for the accelerations of base, first floor and second floor

$$J_7 = \mathrm{NRMS}(\ddot{u}_{bmf}, \ddot{u}_{br}), \tag{47}$$

$$J_8 = \mathrm{NRMS}(\ddot{u}_{1mf}, \ddot{u}_{1r}), \tag{48}$$

$$J_9 = \mathrm{NRMS}(\ddot{u}_{2mf}, \ddot{u}_{2r}), \tag{49}$$

where $\ddot{u}_{\mathrm{br}}$, $\ddot{u}_{1r}$ and $\ddot{u}_{2r}$ are absolute accelerations of the base, first floor and second floor calculated from the reference model. J_4~J_9 are called **global criteria** which is used to evaluate the global RTHS performance compared to the reference model.

5.5 Results and validation

Fig. 18 shows the controller tracking of displacement,

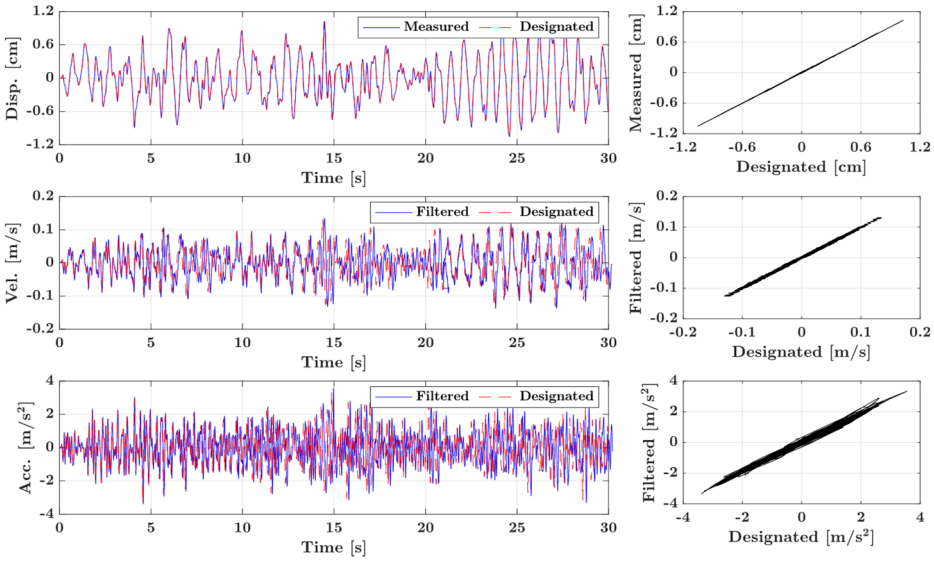

Fig. 18 Controller tracking performance: medium soil and BLWN excitation

Table 5 RTHS evaluation criteria for cases of different excitations and soil types

Exc.	Soil	J_1 [%]	J_2 [%]	J_3 [%]	J_4 [%]	J_5 [%]	J_6 [%]	J_7 [%]	J_8 [%]	J_9 [%]
1	Soft	0.17	1.78	5.16	33.53	22.27	13.30	23.93	33.79	47.38
	Medium	0.13	0.83	1.56	1.86	2.02	3.49	4.15	5.08	5.42
	Dense	0.65	0.32	1.36	1.63	0.67	1.33	7.24	6.27	7.40
2	Soft	0.06	0.35	5.40	17.00	21.53	28.21	21.01	22.04	22.63
	Medium	0.23	0.30	2.24	1.94	3.66	5.51	4.56	4.48	4.57
	Dense	0.61	0.58	4.03	0.67	1.49	4.53	5.15	5.24	5.34

*Note: Exc. means excitation, Exc.1 is BLWN, Exc.2 is El Centro earthquake

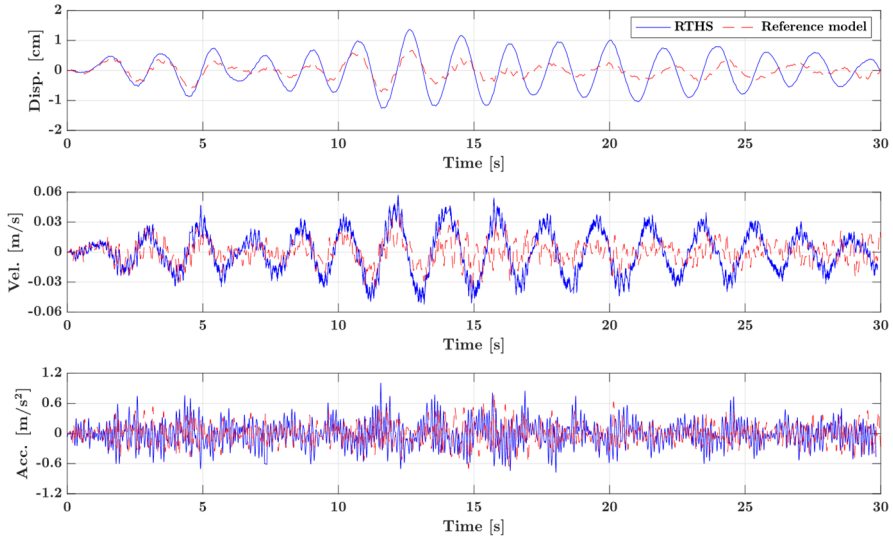

Fig. 19 Foundation (shake table) response: soft soil and BLWN excitation

velocity, and acceleration (from the top to the bottom) for the case of medium soil and BLWN excitation. The right three figures in Fig. 18 show the measured or filtered values against designated values for displacement, velocity, and acceleration, respectively. They are almost straight lines across the origin with slopes nearly of one. The corresponding controller tracking criteria are $J_1 = 0.13\%$, $J_2 = 0.83\%$ and $J_3 = 1.56\%$, indicating good performance of the displacement, velocity, and acceleration tracking.Table 5 provides the values of the evaluation criteria for several cases considering different excitations and soil types. J_1 is no greater than 0.765%, J_2 is no greater than 1.78%, J_3 is

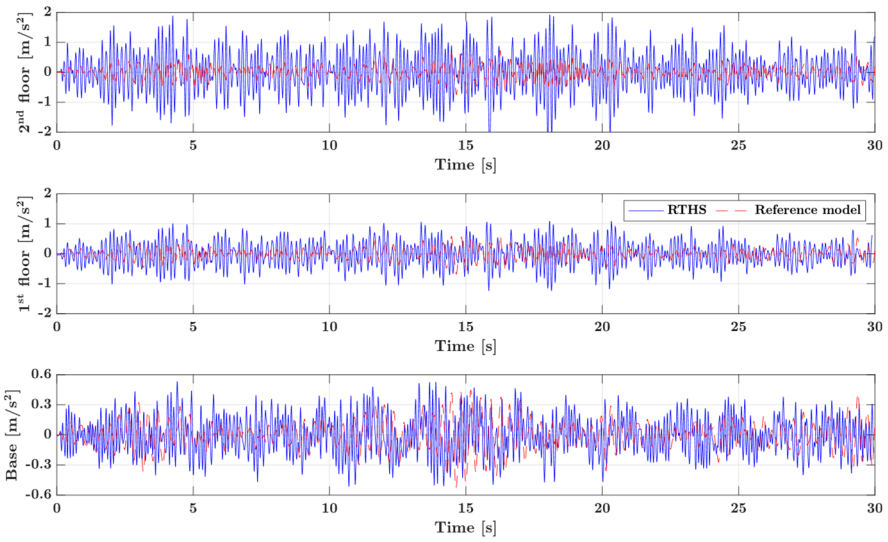

Fig. 20 Frame and base acceleration histories: soft soil and BLWN excitation

no greater than 5.4%. However, the global criteria (J_4~J_9) of soft soil case are much higher (in the range of 17% ~ 47.38%). Thus, the RTHS experiments are not able to characterize the behavior of the reference model for the soft soil case. Time domain responses of RTHS and reference model for the case of BLWN excitation and soft soil are shown in Figs. 19-20. Fig. 19 compares the measured displacement, filtered velocity and filtered acceleration of shake table (foundation) in RTHS with the calculated ones from the reference model, and Fig. 20 compares the filtered accelerations of base, first floor and second floor with calculated accelerations from the reference model.

According to Figs. 19-20, there are much differences between the RTHS and reference model results. By observing the tests for the soft soil case, we found that the shake table and superstructure vibrated rather lightly, and the rolling isolators had almost no relative movements. One reasonable explanation of the poor performance of the soft soil case might be that the friction in the rolling isolators could not be overcome because the base shear is relatively small.

For the medium and dense soil types, some time domain comparisons are provided in Figs. 21-24. Good agreement between the RTHS and reference model can be observed in these time domain responses. The corresponding global criteria lie in the range of 0.67% ~ 7.40%. Two remarks are noted here for the results of medium and dense soil types:

(1) The global criteria (J_4~J_9) have relatively higher values. This behavior indicates that although the controller achieves good tracking performance, the errors between the RTHS and reference model results are still large. The reason might be due to the modelling error in the reference model. Since we divide the system into the base and frame subsystems and identify them separately, the modelling errors might be accumulating. In the base subsystem, the non-conservative forces are simplified as a linear damping force with one parameter c_b, which might cause modeling errors.

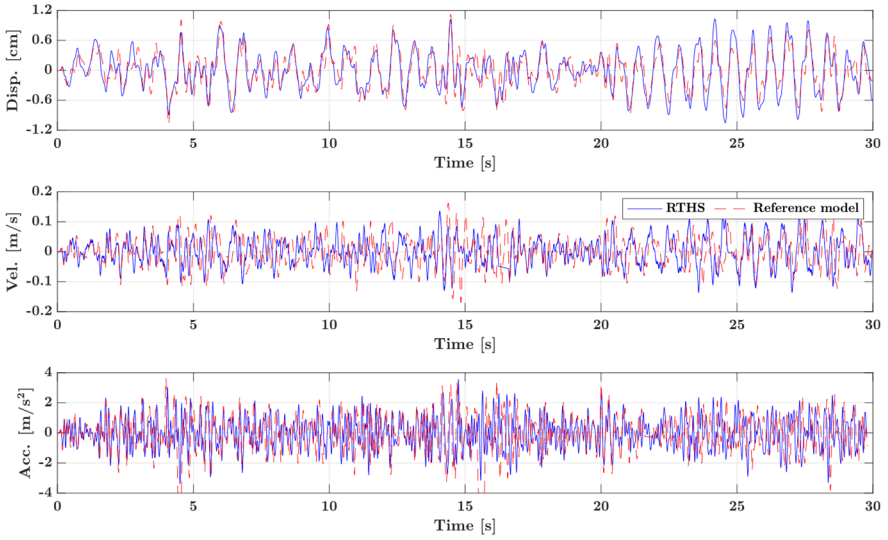

Fig. 21 Foundation (shake table) response: medium soil and BLWN excitation

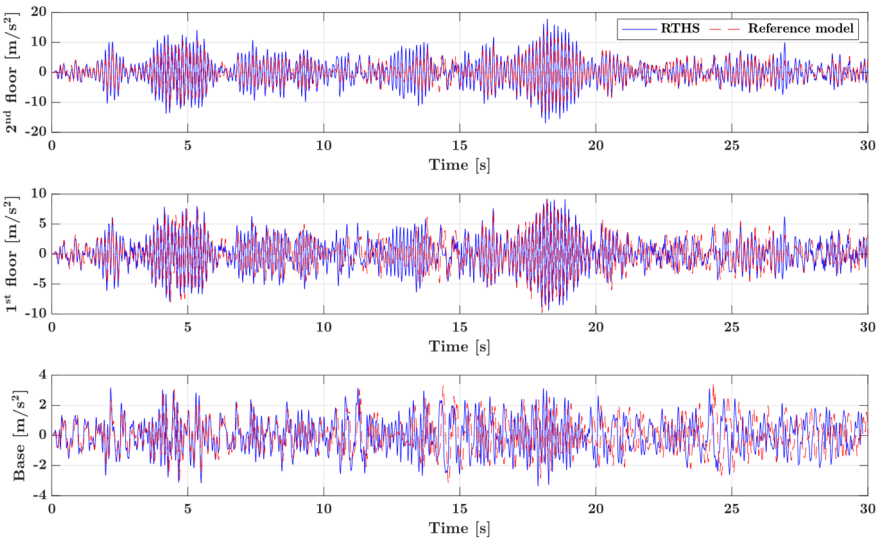

Fig. 22 Frame and base acceleration histories: dense soil and BLWN excitation

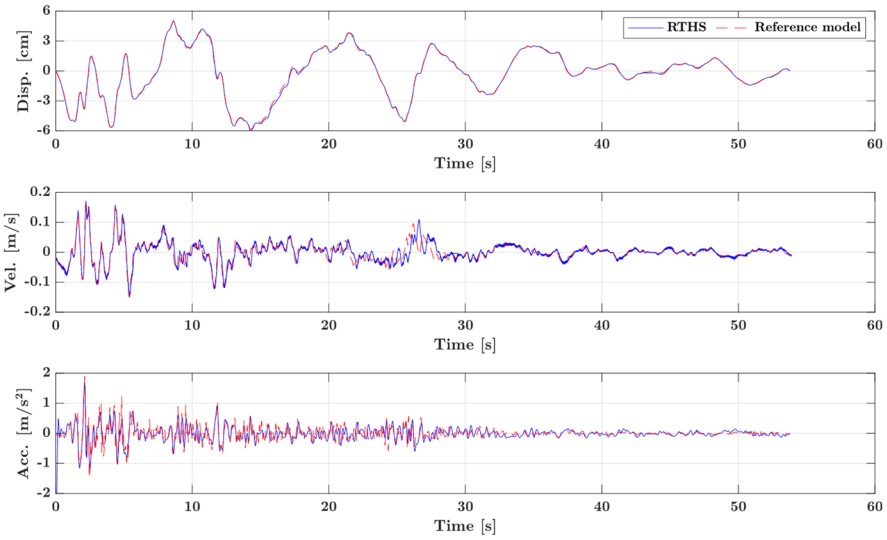

Fig. 23 Foundation (shake table) response: dense soil and El Centro excitation

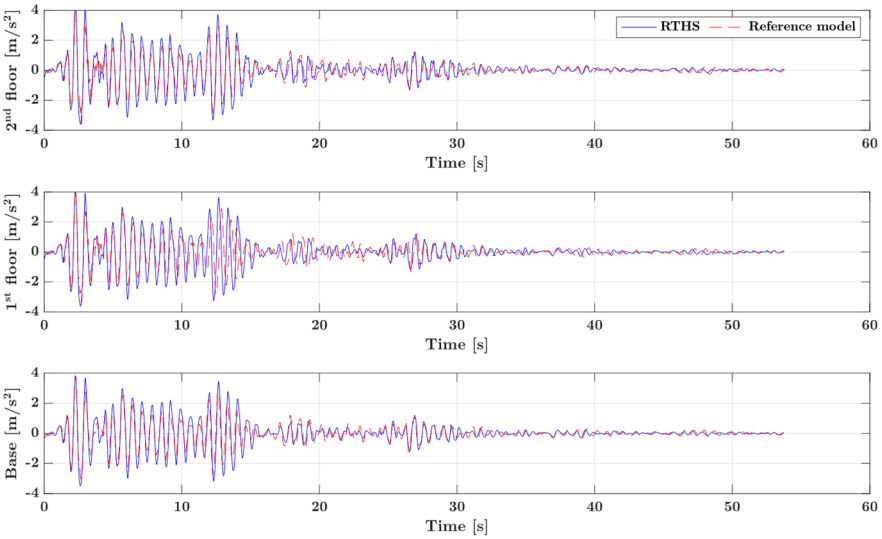

Fig. 24 Frame and base acceleration histories: medium soil and El Centro excitation

And the model of the frame subsystem also contains errors as discussed in Section 4.4.

(2) The values of the global criteria follow a relationship: J_4 (displacement tracking) < J_5 (velocity tracking) < J_6~J_9 (acceleration tracking), which means the higher the order of the tracking variable, the worse the tracking performance. High order responses such as acceleration might be very sensitive to the modelling error in the reference model because the acceleration response contains a wider range of frequency content. This behavior could be a main reason for the high values of the acceleration tracking criteria.

6. Conclusions

In this paper we advance the capacity of RTHS methods as we consider a nonlinear soil-isolator-structure system. Three types of soil (soft, medium, and dense) are considered and captured using the simplified linear sway-rocking model. A band-limited white noise and scaled El Centro earthquake are chosen as ground motions. A shake table serves as the transfer system and is found to exhibit nonlinear behavior due to friction. A sliding mode controller is designed based on the nonlinear shake table model and the uncertainties observed in this transfer system. The controller is tested and validated and shown to have good tracking performance by computing an appropriate set of evaluation criteria, which are no greater than 5.4%.

A nonlinear reference model is established for the system. The reference model behaves similarly as the linearized model at low excitation. However, the differences increase as the magnitude of the excitation increases due to the geometric nonlinearity. Based on the evaluation criteria, the medium and dense soil cases have much better agreement (0.67% ~ 7.4%) with the reference model than the soft soil case (17% ~ 47.38%) does. It is important to note that the system vibrated very lightly and rolling isolators barely moved in the soft soil RTHS case. A possible explanation is the friction in the rolling isolators is not overcome during the tests, leading to the difference compared with the reference model. Despite that, the authors believe that the RTHS of the medium and dense soil cases give reasonable and acceptable results compared to the reference model. The robust RTHS control technique proposed in this paper shows high performance of the shake table displacement, velocity, and acceleration tracking, which raises the possibility for the community to further conduct more complex and realistic SSI studies using RTHS.

Acknowledgments

The authors express their appreciation for the support from the program of China Scholarships Council (No. 201706090092), the Priority Academic Program of Jiangsu Higher Education Institutions (CE02-1-48), the Fundamental Research Funds for the Central University - Postgraduate Research\&Practice Innovation Program of Jiangsu Province (KYCX170126), Distinguished Young Scholars (Grant Number: 51625803), Changjiang Scholars Program of Ministry of Education of China, Distinguished Professor Program of Jiangsu Province, Peruvian National Council of Science Technology and Technological Innovation (CONCYTEC) Fellowship, the US National Science Foundation (Award No. CMMI-1661621) and Purdue University's System Collaboratory Fellows Program.

References

Aldaikh, H., Alexander, N.A., Ibraim, E. and Oddbjornsson, O. (2015), "Two dimensional numerical and experimental models for the study of structure-soil-structure interaction involving three buildings", *Comput. Struct.*, **150**, 79-91. https://doi.org/10.1016/j.compstruc.2015.01.003

Blakeborough, A., Williams, M.S., Darby, A.P. and Williams, D.M. (2001), "The development of real-time substructure testing", *Philos. Trans. R. Soc. Lond. Ser. A-Math. Phys. Eng. Sci.*, **359**(1786), 1869-1891. https://doi.org/10.1098/rsta.2001.0877

Calhoun, S.J. and Harvey, P.S. (2018), "Enhancing the teaching of seismic isolation using additive manufacturing", *Eng. Struct.*, **167**, 494-503. https://doi.org/10.1016/j.engstruct.2018.03.084

Chae, Y., Kazemibidokhti, K. and Ricles, J.M. (2013), "Adaptive time series compensator for delay compensation of servo-hydraulic actuator systems for real-time hybrid simulation", *Earthq. Eng. Struct. Dyn.*, **42**(11), 1697-1715. https://doi.org/10.1002/eqe.2294

Chen, P.C. and Chen, P.C. (2020), "Robust stability analysis of real-time hybrid simulation considering system uncertainty and delay compensation", *Smart. Struct. Syst., Int. J.*, **25**(6), 719-732. http://dx.doi.org/10.12989/sss.2020.25.6.719

Chen, P.C., Hsu, S.C., Zhong, Y.J. and Wang, S.J. (2019), "Real-time hybrid simulation of smart base-isolated raised floor systems for high-tech industry", *Smart. Struct. Syst., Int. J.*, **23**(1), 91-106. http://dx.doi.org/10.12989/sss.2019.23.1.091

Chopra, A.K. (2012). *Dynamics of Structures*: *Theory and Applications to Earthquake Engineering*, (4th Edition), Pearson Education, Inc., Upper Saddle River, NJ, USA.

Condori, J., Maghareh, A., Orr, J., Li, H.W., Montoya, H., Dyke, S., Gill, C. and Prakash, A. (2020), "Exploiting parallel computing to control uncertain nonlinear systems in real-time", *Exp. Tech.*, **44**(6), 735-749. https://doi.org/10.1007/s40799-020-00373-w

Constantinou, M.C. and Kneifati, M.C. (1988), "Dynamics of Soil-Base-Isolated-Structure Systems", *J. Struct. Eng.*, **114**(1), 211-221. https://doi.org/10.1061/(ASCE)0733-9445(1988)114:1(211)

Dyke, S.J., Spencer, B.F., Quast, P. and Sain, M.K. (1995), "Role of control-structure interaction in protective system design", *J. Eng. Mech.*, **121**(2), 322-338. https://doi.org/10.1061/(ASCE)0733-9399(1995)121:2(322)

Ebeido, A., Zayed, M., Kim, K., Wilson, P. and Elgamal, A. (2018), "Large Scale Geotechnical Shake Table Testing at the University of California San Diego", *International Congress and Exhibition*, Cham, Switzerland, November.

Gao, X.Y., Castaneda, N. and Dyke, S.J. (2013), "Real time hybrid simulation: from dynamic system, motion control to experimental error", *Earthq. Eng. Struct. Dyn.*, **42**(6), 815-832. https://doi.org/10.1002/eqe.2246

Ghahari, S.F., Abazarsa, F., Ghannad, M.A. and Taciroglu, E. (2013), "Response-only modal identification of structures using strong motion data", *Earthq. Eng. Struct. Dyn.*, **42**(8), 1221-1242. https://doi.org/10.1002/eqe.2268

Gomez, D., Dyke, S.J. and Maghareh, A. (2015), "Enabling role of hybrid simulation across NEES in advancing earthquake engineering", *Smart Struct. Syst.*, *Int. J.*, **15**(3), 913-929. https://doi.org/10.12989/sss.2015.15.3.913

Gueguen, P. and Bard, P.Y. (2005), "Soil-structure and soil-structure-soil interaction: Experimental evidence at the Volvi test site", *J. Earthq. Eng.*, **9**(5), 657-693. https://doi.org/10.1080/13632460509350561

Guo, J., Tang, Z.Y., Chen, S.C. and Li, Z.B. (2016), "Control strategy for the substructuring testing systems to simulate soil-structure interaction", *Smart Struct. Syst.*, *Int. J.*, **18**(6), 1169-1188. https://doi.org/10.12989/sss.2016.18.6.1169

Harris, C.M. and Piersol, A.G. (2010), *Harris' Shock and Vibration Handbook*, McGraw-Hill, New York, NY, USA.

Harvey, P.S. and Gavin, H.P. (2013), "The nonholonomic and chaotic nature of a rolling isolation system", *J. Sound Vib.*, **332**(14), 3535-3551. https://doi.org/10.1016/j.jsv.2013.01.036

Jangid, R.S. (2005), "Optimum friction pendulum system for near-fault motions", *Eng. Struct.*, **27**(3), 349-359. https://doi.org/10.1016/j.engstruct.2004.09.013

Kabeyasawa, T. (2008), "Nonlinear soil-structure interaction theory for low-rise reinforced concrete buildings based on the full-scale shake table test at E-Defense", *Proceedings of the 14th World Conference on Earthquake Engineering*, Beijing, China, October.

Li, H., Maghareh, A., Montoya, H., Condori, J., Dyke, S. and Xu, Z. (2021), "Sliding mode control design for the benchmark problem in real-time hybrid simulation", *Mech. Syst. Signal Proc.*, **151**, 107364. https://doi.org/10.1016/j.ymssp.2020.107364

Luco, J.E., Trifunac, M.D. and Wong, H.L. (1988), "Isolation of soil-structure interaction effects by full-scale forced vibration tests", *Earthq. Eng. Struct. Dyn.*, **16**(1), 1-21. https://doi.org/10.1002/eqe.4290160102

Maghareh, A., Dyke, S.J., Prakash, A. and Rhoads, J.F. (2014), "Establishing a stability switch criterion for effective implementation of real-time hybrid simulation", *Smart Struct. Syst.*, *Int. J.*, **14**(6), 1221-1245. http://dx.doi.org/10.12989/sss.2014.14.6.1221

Maghareh, A., Dyke, S., Rabieniaharatbar, S. and Prakash, A. (2017), "Predictive stability indicator: a novel approach to configuring a real-time hybrid simulation", *Earthq. Eng. Struct. Dyn.*, **46**(1), 95-116. https://doi.org/10.1002/eqe.2775

Maghareh, A., Dyke, S.J. and Silva, C.E. (2020), "A Self-tuning Robust Control System for nonlinear real-time hybrid simulation", *Earthq. Eng. Struct. Dyn.*, **49**(7), 695-715. https://doi.org/10.1002/eqe.3260

Nakata, N. and Stehman, M. (2014), "Compensation techniques for experimental errors in real-time hybrid simulation using shake tables", *Smart. Struct. Syst.*, *Int. J.*, **14**(6), 1055-1079. http://dx.doi.org/10.12989/sss.2014.14.6.1055

Neethu, B. and Das, D. (2019), "Effect of dynamic soil--structure interaction on the seismic response of bridges with elastomeric bearings", *Asian J. Civ. Eng.*, **20**, 197-207. https://doi.org/10.1007/s42107-018-0098-0

Ou, G., Dyke, S.J. and Prakash, A. (2017), "Real time hybrid simulation with online model updating: An analysis of accuracy", *Mech. Syst. Signal Proc.*, **84**, 223-240. https://doi.org/10.1016/j.ymssp.2016.06.015

Pais, A. and Kausel, E. (1988), "Approximate formulas for dynamic stiffnesses of rigid foundations", *Soil Dyn. Earthq. Eng.*, **7**(4), 213-227. https://doi.org/10.1016/S0267-7261(88)80005-8

Pioldi, F., Salvi, J. and Rizzi, E. (2017), "Refined FDD modal dynamic identification from earthquake responses with Soil-Structure Interaction", *Int. J. Mech. Sci.*, **127**, 47-61. https://doi.org/10.1016/j.ijmecsci.2016.10.032

Slotine, J.E. and Li, W. (1991). *Applied Nonlinear Control*, Prentice Hall, Englewood Cliffs, NJ, USA.

Spyrakos, C.C., Koutromanos, I.A. and Maniatakis, C.A. (2009), "Seismic response of base-isolated buildings including soil-structure interaction", *Soil Dyn. Earthq. Eng.*, **29**(4), 658-668. https://doi.org/10.1016/j.soildyn.2008.07.002

Todorovska, M.I. (2002), "Full-scale experimental studies of soil-structure interaction", *ISET J. Earthq. Technol.*, **39**(3), 139-165. https://cpb-us-e1.wpmucdn.com/sites.usc.edu/dist/f/100/files/2018/03/7-1h10zxx.pdf#page=236

Tsai, C.S., Hsueh, C.I. and Su, H.C. (2016), "Roles of soil-structure interaction and damping in base-isolated structures built on numerous soil layers overlying a half-space", *Earthq. Eng. Eng. Vib.*, **15**(2), 387-400. https://doi.org/10.1007/s11803-016-0331-3

Wang, Q., Wang, J.T., Jin, F., Chi, F.D. and Zhang, C.H. (2011), "Real-time dynamic hybrid testing for soil-structure interaction analysis", *Soil Dyn. Earthq. Eng.*, **31**(12), 1690-1702. https://doi.org/10.1016/j.soildyn.2011.07.004

Wang, Z., Wu, B., Bursi, O.S., Xu, G.S. and Ding, Y. (2014), "An effective online delay estimation method based on a simplified physical system model for real-time hybrid simulation", *Smart Struct. Syst.*, *Int. J.*, **14**(6), 1247-1267. http://dx.doi.org/10.12989/sss.2014.14.6.1247

Zhang, R.Y., Lauenstein, P.V. and Phillips, B.M. (2016), "Real-time hybrid simulation of a shear building with a uni-axial shake table", *Eng. Struct.*, **119**, 217-229. https://doi.org/10.1016/j.engstruct.2016.04.022

Zhang, R.Y., Phillips, B.M., Taniguchi, S., Ikenaga, M. and Ikago, K. (2017), "Shake table real-time hybrid simulation techniques for the performance evaluation of buildings with inter-story isolation", *Struct. Control. Health Monit.*, **24**(10). https://doi.org/10.1002/stc.1971

Zhou, M.X., Wang, J.T., Jin, F., Gui, Y. and Zhu, F. (2014), "Real-Time Dynamic Hybrid Testing Coupling Finite Element and Shaking Table", *J. Earthqu. Eng.*, **18**(4), 637-653. https://doi.org/10.1080/13632469.2014.897276

Zhuang, H.Y., Fu, J.S., Yu, X., Chen, S. and Cai, X.H. (2019), "Earthquake responses of a base-isolated structure on a multi-layered soft soil foundation by using shaking table tests", *Eng. Struct.*, **179**, 79-91. https://doi.org/10.1016/j.engstruct.2018.10.060

BS